Cell Death and Differentiation (2017) 24, 523–533
© 2017 Macmillan Publishers Limited, part of Springer Nature. All rights reserved 1350-9047/17

www.nature.com/cdd

The BCL-2 pro-survival protein A1 is dispensable for T cell homeostasis on viral infection

Selma Tuzlak[1,2,5], Robyn L Schenk[2,3,5], Ajithkumar Vasanthakumar[2,3], Simon P Preston[2,3], Manuel D Haschka[1], Dimitra Zotos[2,3], Axel Kallies[2,3], Andreas Strasser[2,3], Andreas Villunger[1,4] and Marco J Herold[*,2,3]

The physiological role of the pro-survival BCL-2 family member A1 has been debated for a long time. Strong mRNA induction in T cells on T cell receptor (TCR)-engagement suggested a major role of A1 in the survival of activated T cells. However, the investigation of the physiological roles of A1 was complicated by the quadruplication of the *A1* gene locus in mice, making *A1* gene targeting very difficult. Here, we used the recently generated *A1*$^{-/-}$ mouse model to examine the role of A1 in T cell immunity. We confirmed rapid and strong induction of A1 protein in response to TCR/CD3 stimulation in CD4^{+} as well as CD8^{+} T cells. Surprisingly, on infection with the acute influenza HKx31 or the lymphocytic choriomeningitis virus docile strains mice lacking A1 did not show any impairment in the expansion, survival, or effector function of cytotoxic T cells. Furthermore, the ability of *A1*$^{-/-}$ mice to generate antigen-specific memory T cells or to provide adequate CD4-dependent help to B cells was not impaired. These results suggest functional redundancy of A1 with other pro-survival BCL-2 family members in the control of T cell-dependent immune responses.

Cell Death and Differentiation (2017) **24,** 523–533; doi:10.1038/cdd.2016.155; published online 13 January 2017

On antigenic challenge, T lymphocytes need to rapidly switch from their IL-7/IL-7R-regulated naive, quiescent state[1,2] to a T cell antigen-receptor (TCR/CD3) stimulation-induced activation state.[3] In case of inappropriate stimulation of the TCR, for example, in the absence of co-receptor stimulation, this shift in the survival programme is not induced and leads to rapid T cell death.[4] Conversely, appropriately stimulated T cells expand rapidly, allowing accumulation of T cell clones expressing TCRs of high affinity for specific antigens. During this clonal expansion, BCL-2 family regulated apoptosis acts as a mechanism to remove low-affinity T cells, thereby ensuring the generation of a highly effective immune response.[5] On infection clearance, most of the activated T cells are removed by apoptosis,[6] leaving only some T cells with antigen-specific high-affinity TCRs in reserve as long-lived memory T cells.[7]

The BCL-2 family of proteins regulate apoptotic cell death, with the balance between pro-survival and pro-apoptotic family members determining whether a cell lives or dies. The expression of pro-survival BCL-2 family members is dynamically regulated during T cell activation.[8] TCR/CD3 ligation leads to the downregulation of BCL-2 and induction of BCL-XL.[3] Accordingly, *Bcl-2*$^{-/-}$ mice display a loss of mature, unstimulated T cells, and the death of these cells can be prevented by TCR/CD3 stimulation.[9] Interestingly, although BCL-XL is substantially upregulated on TCR/CD3 stimulation, its loss did not increase apoptosis or impair proliferation of T cells stimulated with mitogenic antibodies.[10] In contrast, MCL-1 has been shown to be a crucial pro-survival factor after T cell activation.[11,12] A1 is a pro-survival BCL-2 family protein that has been proposed to be important for activated T cell survival based on its expression status in different T cell subsets. In naive T cells, A1 protein is hardly detectable, but its expression is strongly and rapidly induced on TCR/CD3 stimulation.[3,13]

Addressing the physiological role of A1 in mice has been difficult due to a quadruplication of the *Bcl2a1* locus in the mouse genome.[14] *A1*-knockdown studies using *in vivo* expression of shRNAs in the haematopoietic system suggested a role for A1 in mast cell maturation,[15] mature B cell survival[8] and early T cell development,[16] although not all of these phenotypes were found across the different mouse models analysed. To unambiguously determine the functions of A1, we developed an *A1* knockout mouse strain in which all three functional paralogues of *A1* (*A1-a*, *A1-b* and *A1-d*) had been deleted.[17] Interestingly, these *A1*-deficient mice show little to no abnormalities under steady state conditions. However, these observations might not be totally surprising, given that A1 protein levels are very low in unstimulated cells.[18] Therefore, we investigated a role for A1 in mice that had been challenged with different viral infections. These studies clearly demonstrate that loss of A1 alone does not impair T cell-driven immune responses. It therefore appears likely that A1 has critical overlapping functions with other pro-survival BCL-2 proteins in T cell immune responses.

[1]Division of Developmental Immunology, BIOCENTER, Medical University Innsbruck, Innsbruck, Austria; [2]The Walter & Eliza Hall Institute for Medical Research, Parkville, Melbourne, VIC 3052, Australia; [3]Department of Medical Biology, University of Melbourne, Parkville, Melbourne, VIC 3050, Australia and [4]Tyrolean Cancer Research Institute, Innsbruck, Austria

*Corresponding author: MJ Herold, Walter & Eliza Hall Institute for Medical Research, 1G Royal Parade, Parkville, Melbourne, VIC 3050, Australia. Tel: 61 3 9345 2497; Fax: 61-3-9347-0852; E-mail: herold@wehi.edu.au

[5]These authors contributed equally to this work.

Received 14.7.16; revised 08.11.16; accepted 01.12.16; Edited by C Borner; published online 13.1.2017

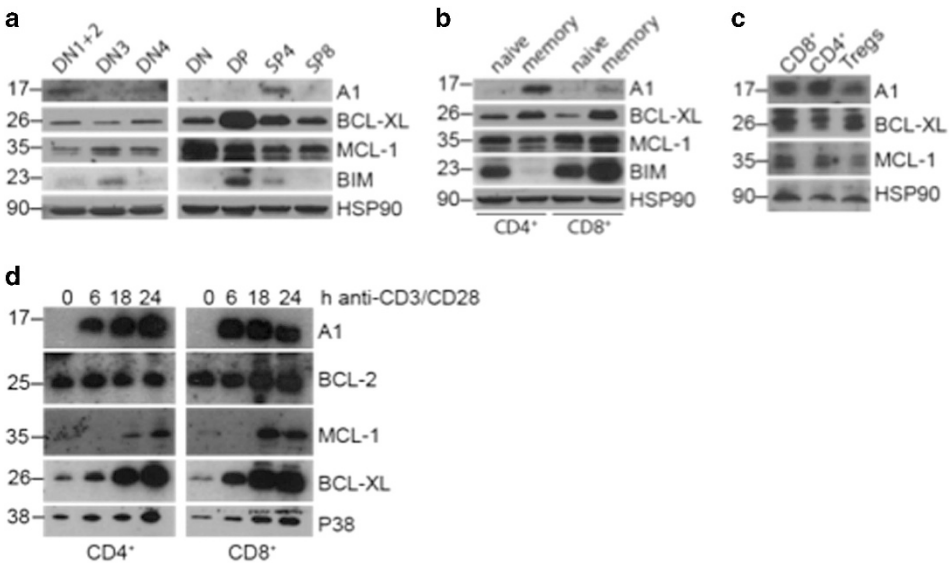

Figure 1 *A1* is mainly expressed in SP4 thymocytes and memory T cells and is rapidly upregulated in T cells on TCR/CD3 stimulation. (**a**) $CD4^-CD8^-CD44^+$ double-negative stage (DN)1 and DN2, $CD4^-CD8^-CD25^+CD44^-$ DN3, $CD4^-CD8^-CD44^-CD25^-$ DN4, $CD4^-CD8^-$ total DN, $CD4^+CD8^+$ DP, $CD4^+CD8^-$ single CD4 positive (SP4) and $CD4^-CD8^+$ (SP8) wild-type thymocytes were FACS-sorted and lysed in NP-40 containing lysis buffer. Western blots were probed for the proteins indicated. Probing for HSP90 served as loading control. (**b**) Naive ($CD62L^+CD44^-$) and memory-like ($CD62L^-CD44^+$) $CD4^+$ or $CD8^+$ T cells were sorted from wild-type splenocytes and treated as described in (**a**). (**c**) 8.5×10^5 $CD8^+$, $CD4^+FOXP3^-$ conventional T cells and $CD4^+FOXP3^+$ regulatory T cells (Tregs), respectively, were FACS-sorted from $Foxp3^{YFP\text{-}cre}$ mice according to their expression of CD8, CD4 and YFP. Cells were lysed directly in 1 × Laemmli buffer for western blot analysis. (**d**) $CD4^+$ (left graph) or $CD8^+$ (right graph) T cells were sorted from spleens of wild-type mice and activated *in vitro* with 5 μg/ml plate-bound anti-CD3 and 1 μg/ml anti-CD28 antibodies for the indicated times. Cells were lysed and western blot analysis performed for the indicated proteins. Membranes were probed with an antibody specific for p38 MAPK to control for equal protein loading. Western blots shown are representative of two independent experiments

Results

***A1* is predominantly expressed in CD4-single positive thymocytes and memory T cells and is rapidly upregulated on TCR/CD3 stimulation.** A1 expression was reported on pre-TCR signalling[19] as well as in double-positive (DP) thymocytes,[20] and is massively induced on T cell activation.[13] Owing to the absence of a reliable antibody detecting murine A1 at that time, these observations were based mainly on mRNA expression analysis. To test A1 protein levels in thymocyte subsets, we isolated them according to their expression of cell subset markers and performed western blot analysis on these extracts. We could detect robust A1 protein expression only in DN1 and 2 and in SP4 thymocytes and to a lesser extent in DN4 stage thymocytes (Figure 1a). This was consistent with our quantitative real-time PCR (qRT-PCR) results (Supplementary Figure 1A). As described previously, BCL-XL expression was highest in DP thymocytes and MCL-1 was expressed throughout all T cell developmental stages. In mature $CD4^+$ and $CD8^+$ splenic T cells, A1 was predominantly expressed in $CD62L^-CD44^+$ memory-like T cells but was barely detectable in naive T cells (Figure 1b), agreeing with our qRT-PCR data (Supplementary Figure 1B). Interestingly, less A1 protein was detected in $FoxP3^+$ Tregs compared with conventional T cells (Figure 1c).

Furthermore, we isolated $CD4^+$ and $CD8^+$ T cells from the spleens of wild-type mice and stimulated them in culture with anti-CD3 and anti-CD28 to mimic antigenic activation. We confirmed rapid A1 induction at the protein (Figure 1d) as well as the mRNA level (Supplementary Figure 1C). Regarding the other pro-survival BCL-2 family members, BCL-2 protein and mRNA levels did not change after TCR/CD3 stimulation, while the amount of MCL-1 protein increased. BCL-XL mRNA and protein levels both increased over the time of TCR/CD3 stimulation, although at a slower rate compared with A1 (Figure 1d and Supplementary Figure 1C).

These findings reveal that A1 is weakly expressed throughout T cell development in the thymus and in resting peripheral T cells but is upregulated on antigen-receptor stimulation.

***A1*$^{-/-}$ T cells show normal responses on acute infection with influenza virus in a haematopoietic chimaeric setting.** As A1 expression was rapidly induced in T cells on activation, we investigated whether the lack of A1 would impair T cell immune responses in a viral infection model. To avoid possible premature death of *A1*$^{-/-}$ mice due to impaired anti-viral immunity, we generated mixed bone-marrow chimaeric mice (C57BL/6-Ly5.1 wild-type: C57BL/6-Ly5.2 *A1*$^{-/-}$ 1:1) and infected them intra-nasally with the influenza strain HKx31 (Figure 2a). Another advantage of mixed bone-marrow chimaeras is that we can detect putative competitive disadvantages of *A1*$^{-/-}$ lymphoid cells on activation and can therefore directly compare wild-type and *A1*$^{-/-}$ T cells responding to viral challenge within the same animal. After 8 days of infection, lungs, mediastinal LN (mLN), and spleens were isolated and analysed by flow cytometry. First, we compared the Ly5.1 to Ly5.2 ratio among $CD4^+$ T cells, $CD8^+$ T cells, and B cells in the spleen to the respective cell types in the blood 5 weeks after reconstitution.

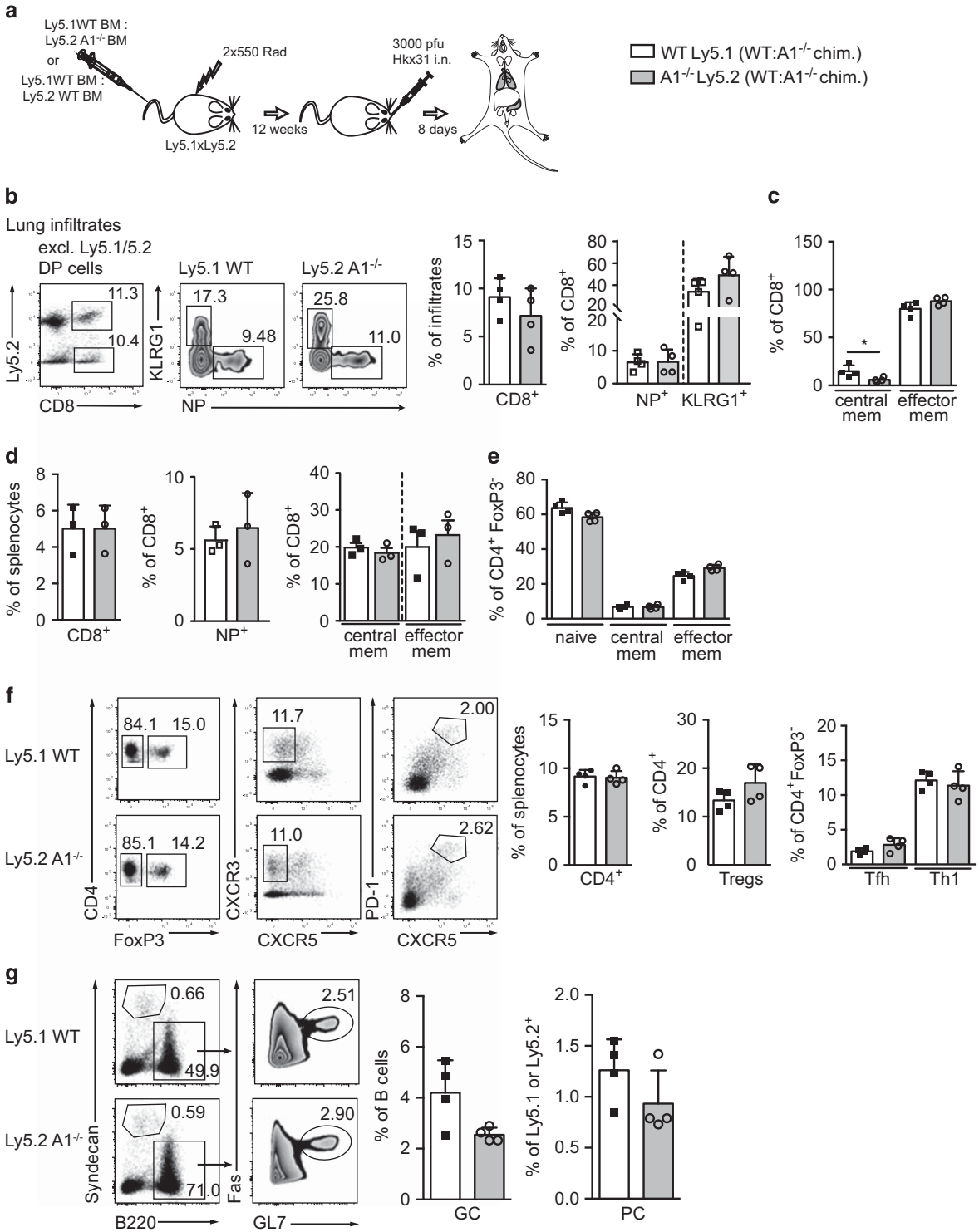

Figure 2 *A1*$^{-/-}$ cells in chimaeric mice exhibit normal T cell immune responses in an acute influenza infection model. (**a**) Schematic overview of the influenza infection workflow: C57BL/6-Ly5.1xLy5.2 F1 mice were lethally irradiated and reconstituted with 1:1 mixed bone-marrow from C57BL/6-Ly5.1 wild-type and C57BL/6-Ly5.2 *A1*$^{-/-}$ mice. Reconstituted mice were infected intra-nasally (i.n.) with 3000 pfu HKx31 influenza virus and lungs and spleens were analysed 8 days post infection by flow cytometry. (**b**) Leukocyte infiltrates were isolated from lungs of chimaeric mice by gradient centrifugation. The recovered cells were analysed by flow cytometry for tetramer-positive antigen-specific (NP$^+$) CD8$^+$ T cells, KLRG1$^+$ short-lived CD8$^+$ effector T cells and (**c**) central (CD44$^+$CD62L$^+$) as well as effector (CD44$^+$CD62L$^-$) memory-like CD8$^+$ T cells. (**d**) Spleen cells from infected bone-marrow chimaeric mice were isolated and analysed for CD8$^+$ NP$^+$ cells, or central as well as effector memory-like CD8$^+$ T cells. (**e**) CD4$^+$ splenic T cells were further analysed for CD4$^+$FoxP3$^-$ naive (CD62L$^+$CD44-), central or effector memory-like subsets. (**f**) CD4$^+$ splenic T cells were analysed for FoxP3$^+$ Treg cells, FoxP3$^-$CXCR3$^+$ Th1 cells, and FoxP3$^-$CXCR5$^+$PD-1$^+$ Tfh cells. (**g**) Spleen cells from infected mice were analysed for Syndecan1$^+$ plasma cells (PC) and B220$^+$FAS$^+$GL7$^+$ germinal centre B cells (GC). Bars represent means ± S.E.M. ($n = 4$), irradiation-resistant Ly5.1/5.2 DP cells were excluded by electronic gating

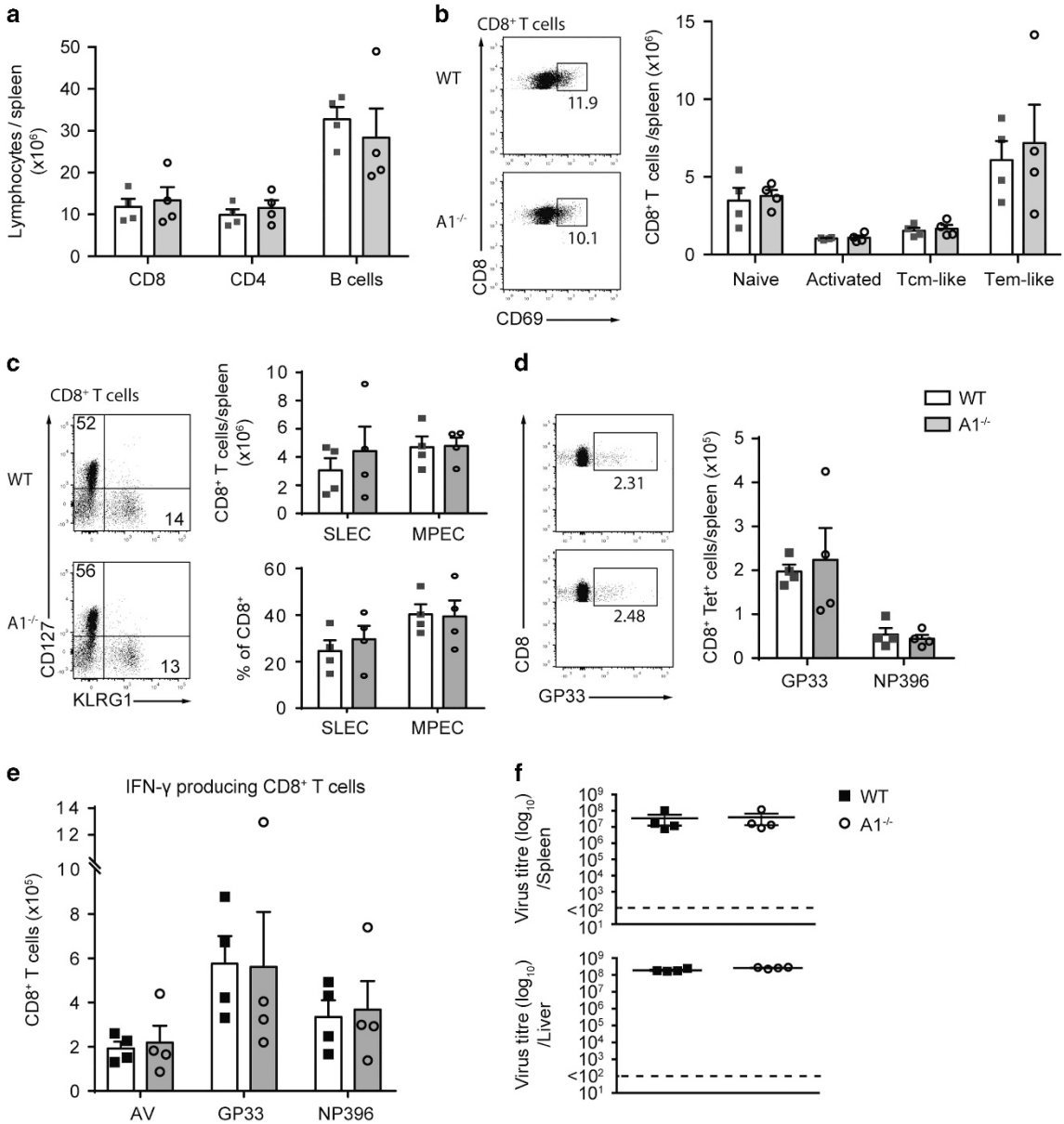

Figure 3 *A1*$^{-/-}$ mice exhibit normal T cell immune responses to chronic infection with LCMV docile. Wild-type and *A1*$^{-/-}$ mice were infected i.v. with 2×10^6 pfu LCMV docile and spleens were analysed 8 days post infection by flow cytometry. (**a**) Total numbers of CD8$^+$ as well as CD4$^+$ T cells and B cells were assessed by cell counting and flow cytometric analysis. (**b**) CD8$^+$ T cells were further analysed for CD62L$^+$CD44$^-$ naive, CD69$^+$ activated, CD44$^+$CD62L$^+$ central memory (Tcm) like, CD44$^+$CD62L$^-$ effector memory (Tem) like T cells. (**c**) CD8$^+$ T cells were also analysed for CD127-KLRG1$^+$ short-lived effector cells (SLEC) and CD127$^+$KLRG1$^-$ memory precursor effector cells (MPEC). (**d**) The numbers of GP33$^+$ low-affinity antigen-specific, or NP396$^+$ high-affinity antigen-specific CD8$^+$ T cells were assessed. (**e**) Spleen cells from infected mice were cultured in the presence of adenovirus, GP33, or NP396 antigen overnight and intracellular staining for IFN-γ was performed and cells analysed by flow cytometry. (**f**) LCMV titres were calculated from spleens and livers of infected mice 8 days post infection. Bars represent means $\pm$ S.E.M. ($n = 4$)

A1$^{-/-}$ haematopoietic stem cells did not show any disadvantage in reconstituting the above mentioned cell lineages and the ratios between the *A1*$^{-/-}$ cells and their competitors remained stable over the observation time (Supplementary Figure 2A). Leukocyte infiltrates were isolated from the lung by gradient centrifugation and analysed for CD8$^+$ cytotoxic T cells (CTLs). Ly5.1/Ly5.2 DP T cells originating from the host were gated out to allow visualisation only of the *A1*$^{-/-}$ and wild-type competitor donor-derived cells. No differences were observed in the frequencies of CTLs of wild-type *versus* *A1*$^{-/-}$ origin (Figure 2b). Furthermore, antigen-specific CD8$^+$NP$^+$ CTLs of wild-type *versus* *A1*$^{-/-}$ origin did not differ in their numbers and frequencies (Figure 2b). *A1*$^{-/-}$ derived short-lived effector CTLs were found to be slightly increased (Figure 2b). However, a similar trend was observed when WT-Ly5.1:WT-Ly5.2 mixed bone-marrow chimaeras were analysed. This might suggest an advantage of Ly5.2$^+$ cells in this T cell subset (Supplementary Figure 2B). A1-deficient

lung infiltrating CTLs contained fewer central memory-like T cells (T_{CM}) compared with those of wild-type origin. However, a similar tendency was seen in WT-Ly5.2$^+$: WT-Ly5.1$^+$ reconstituted mice (Supplementary Figure 2A). Importantly, the numbers of the most abundant T cell subset in the lungs, the effector-like memory T cells (T_{EM}), were comparable between *A1*$^{-/-}$ and wild-type origin (Figure 2c).

Moreover, the frequencies of total CTLs in the spleen was comparable between the wild-type and *A1*$^{-/-}$ compartments (Figure 2d). Approximately 5% of CTLs were NP-specific for both the T cells of *A1*$^{-/-}$ and wild-type origin (Figure 2d). In addition, the frequencies of T_{EM} and T_{CM} CTLs were comparable between those of *A1*$^{-/-}$ and wild-type origin (Figure 2d).

Similarly, *A1*$^{-/-}$ and wild-type haematopoietic stem cell derived CD4$^+$ T cells showed comparable frequencies of T_{CM} and T_{EM} (Figure 2e). Furthermore, no differences in regulatory T cells (Tregs), Type-1 helper cells (Th1) and follicular T helper cells (Tfh) were observed for T-lymphoid cells derived from *A1*$^{-/-}$ or wild-type in the spleen (Figure 2f). Moreover, GC B cell and PC formation appeared normal in the *A1*$^{-/-}$ compartment when compared with their wild-type counterparts (Figure 2g).

Collectively, these findings show that *A1*$^{-/-}$ lymphocytes are able to mount a normal immune response to infection with influenza even in competition with wild-type T cells within the same animal. Apart from a slight reduction in lung infiltrating T_{CM} in the *A1*$^{-/-}$ population compared with their wild-type counterparts, no impact of loss of A1 could be observed in any haematopoietic cell type analysed.

***A1*$^{-/-}$ mice show normal T cell immune responses to chronic infection with lymphocytic choriomeningitis virus docile.** Next, we examined the impact of A1-deficiency on T cell immune responses in a chronic virus infection model. *A1*$^{-/-}$ and wild-type mice were infected with lymphocytic choriomeningitis virus (LCMV) docile, which cannot be cleared and eventually leads to exhaustion of CTLs.[21] Eight days post infection, mice were killed and their spleens analysed. The total cellularity of the spleens was comparable between wild-type and *A1*$^{-/-}$ mice (Supplementary Figure 3A), and we clearly observed an enrichment of CTLs in mice of both genotypes (Figure 3a and Supplementary Figure 3B). Next, we analysed the activation profile of T cells from the infected animals. T_{EM}-like cells were most abundant within the CTL pool. Loss of A1 had no impact on their numbers (Figure 3b) or frequencies (Supplementary Figure 3C). Moreover, *A1*$^{-/-}$ CD4$^+$ T cells did not show any alterations in their memory compartment compared with infected wild-type mice (Supplementary Figure 3D). *A1*$^{-/-}$ mice displayed a slight reduction in B cells on infection and a tendency towards a compensatory increase in granulocytes and macrophages (Supplementary Figure 3B).

CTLs can be further characterised based on their expression of KLRG1 and the IL-7 receptor alpha chain (CD127) into short-lived effector cells (SLECs, CD8$^+$KLRG1$^+$CD127$^-$) and memory precursor effector cells (MPECs, CD8$^+$KLRG1$^-$ CD127$^+$). Although A1 is mainly expressed in memory T cells (Figure 1), *A1*$^{-/-}$ and wild-type CTLs contained similar frequencies and numbers of SLECs and MPECs (Figure 3c).

Next, we analysed antigen-specific CTLs by staining with class I MHC tetramers loaded with GP33 or NP396 peptides; allowing discrimination between low-affinity and high-affinity antigen-specific T cells, respectively. No differences in the numbers and frequencies of low- or high-affinity CTLs could be observed between infected *A1*$^{-/-}$ and wild-type mice (Figure 3d and Supplementary Figure 3E). To assess whether A1-deficient antigen-specific T cells were capable of producing IFN-*γ* in an *in vitro* recall response, total splenocytes from infected animals were stimulated overnight with GP33 or NP396 peptides before cytokine production was analysed by intracellular flow cytometry. No differences in the frequencies and numbers of IFN-*γ*-producing T cells was observed between splenocytes from infected *A1*$^{-/-}$ *versus* wild-type mice (Figure 3e and Supplementary Figure 3F). Finally, we analysed the load of LCMV in the spleen, liver, kidney, lung and brain of infected mice. No differences in viral titres were noted between wild-type and *A1*$^{-/-}$ mice (Figure 3f and Supplementary Figure 3G).

On the basis of these findings we conclude that loss of A1 does not impair the activation or expansion of CTLs in a chronic infection model of LCMV Docile.

A1-deficient T cells show normal memory responses and expand normally on repeated challenge with influenza virus *in vivo*. In a separate study, we found that unchallenged *A1*$^{-/-}$ mice have slightly reduced numbers of memory T cells compared with their wild-type counterparts.[17] Therefore, we analysed the impact of A1-deficiency in memory T cell formation. Hence, mice were infected intra-nasally with influenza HKx31 virus and memory T cells were enumerated 41 days after infection. First, we analysed the intrinsic ability of *A1*$^{-/-}$ CTLs to generate long-lived memory T cells by infecting BM chimaeras (Figure 4 and Supplementary Figure 4). After 41 days, comparable frequencies of antigen-specific memory CTLs could be found in the wild-type and *A1*$^{-/-}$ compartments (Figure 4a). Furthermore, the frequencies of *A1*$^{-/-}$ T_{CM} and T_{EM} CTLs were comparable (Figure 4a), as were the frequencies of Tregs (Figure 4b).

To test for possible extrinsic effects on CD8$^+$ memory T cell formation, intact *A1*$^{-/-}$ and wild-type mice were infected with influenza virus. No differences in the memory profile of CTLs in the spleen (Figure 4c) were observed. Moreover, the numbers of NP-specific CTLs were equivalent between the infected wild-type and *A1*$^{-/-}$ mice (Figure 4d). Finally, loss of A1 did not appear to impair the development of CD4$^+$ memory T cells (Figure 4e).

Next, we investigated whether A1 has a role in the reactivation of memory T cells. C57BL/6-Ly5.2$^+$ wild-type and *A1*$^{-/-}$ mice were infected with influenza virus and killed after 41 days. CTLs were enriched by magnetic bead purification and 2×10^4 NP-specific A1-deficient or wild-type T cells were transferred into naive C57BL/6-Ly5.1$^+$ (wild-type) recipient mice (Figure 5a). These mice were challenged with influenza virus one day later and analysed 8 days post infection. We readily identified Ly5.2$^+$ donor-derived T cells in the spleen, mLN and lungs. No differences were observed between mice transplanted with either wild-type or *A1*$^{-/-}$ memory T cells (Figure 5b). In the lungs ~20% of the

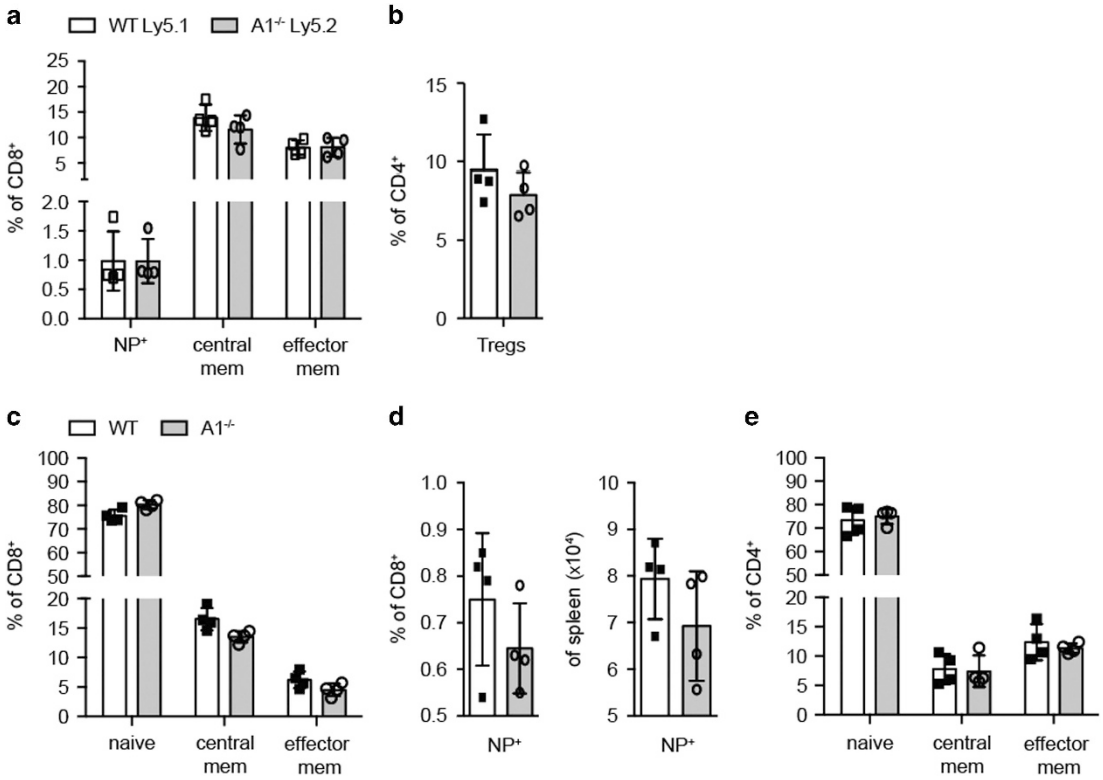

Figure 4 *A1*$^{-/-}$ T cells show normal *in vivo* memory formation. (**a**) 1 : 1 C57BL/6-Ly5.1 wild-type and C57BL/6-Ly5.2 *A1*$^{-/-}$ bone-marrow chimaeric mice were infected i.n. with 3000 pfu HKx31 influenza virus and spleen cells were analysed 41 days post infection by flow cytometry. CD8$^+$ T cells were analysed for NP$^+$ antigen-specific T cells as well as for central memory and effector memory-like phenotypes. (**b**) The frequencies of Treg cells within the CD4$^+$ T cell population were analysed by intracellular flow cytometry for FoxP3 expression. (**c**) Wild-type and *A1*$^{-/-}$ mice were infected i.n. with 3000 pfu HKx31 influenza virus and spleen cells were analysed 41 days post infection by flow cytometry. CD8$^+$ T cell populations were analysed for naive, central memory, and effector memory T cells. (**d**) The frequencies and total numbers of NP$^+$ antigen-specific CD8$^+$ T cells were assessed by flow cytometry. (**e**) CD4$^+$ T cells in the spleens of infected mice were analysed for naive, central memory, and effector memory T cells. Bars represent means ± S.E.M. ($n=4$)

infiltrating leukocytes were Ly5.2$^+$ donor-derived CTLs (Figure 5b), and this frequency was comparable to the Ly5.1$^+$ infiltrates that were derived from a primary infection (Ly5.1$^+$host, Supplementary Figure 5A). Approximately 30% of Ly5.2$^+$ wild-type and Ly5.2 *A1*$^{-/-}$ CTLs were antigen-specific (Figure 5c), indicating a strong memory response. The expansion of total NP$^+$CTLs was calculated by comparing the number of injected NP$^+$CTLs to the number recovered from spleen, mLN and lung. No differences were observed between the two genotypes (Figure 5d).

To rule out that other pro-survival BCL-2 family members were upregulated to compensate for the loss of A1, BCL-2 and MCL-1 protein levels were determined by intracellular flow cytometry in Ly5.2$^+$wild-type, Ly5.2$^+$*A1*$^{-/-}$ donor-derived CTLs and Ly5.1$^+$wild-type host CTLs. No evidence of upregulation of BCL-2 or MCL-1 in *A1*$^{-/-}$ CTLs was observed at the time points tested (Figure 5e). We were unable to assess BCL-XL by flow cytometry due to the relatively poor quality of these antibodies. Moreover, these cells could not be isolated in sufficient numbers to perform Western blot analysis. Interestingly, Ly5.2 wild-type CTLs showed a slight increase in MCL-1 protein levels, which was not observed in *A1*$^{-/-}$ CTLs. BCL-2 expression was reduced in both Ly5.2$^+$ wild-type and *A1*$^{-/-}$ CTLs.

Collectively, these findings demonstrate that A1 is dispensable for CD8$^+$ memory T cell formation, expansion and function.

T-helper cell function and B cell responses are not impaired in *A1*$^{-/-}$ mice immunised with NP-KLH/Alum. Influenza and LCMV infection primarily activate CTLs, but CD4$^+$ T-helper cells and B cells also participate in the clearance of viruses and other pathogens.[22] To address whether A1 might have an impact on Tfh cells or the formation of GC B cells and long-lived PC, *A1*$^{-/-}$ and wild-type mice were immunised with NP-KLH/Alum and analysed 14 days later by flow cytometry. Total spleen cellularity was similar between wild-type and *A1*$^{-/-}$ mice (Figure 6a). The total numbers of Tfh were slightly although not significantly reduced in *A1*$^{-/-}$ mice (Figure 6b). The frequencies and numbers of antigen-specific Ig class-switched GC B cells were comparable between immunised *A1*$^{-/-}$ and wild-type mice (Figure 6c). This indicates that the slight reduction of Tfh cells observed in *A1*$^{-/-}$ mice might not be physiologically relevant. The total numbers of PC were slightly but not significantly reduced in the immunised A1-deficient mice compared with their wild-type counterparts (Figure 6d). To enumerate the antigen-specific PC in the spleen and bone

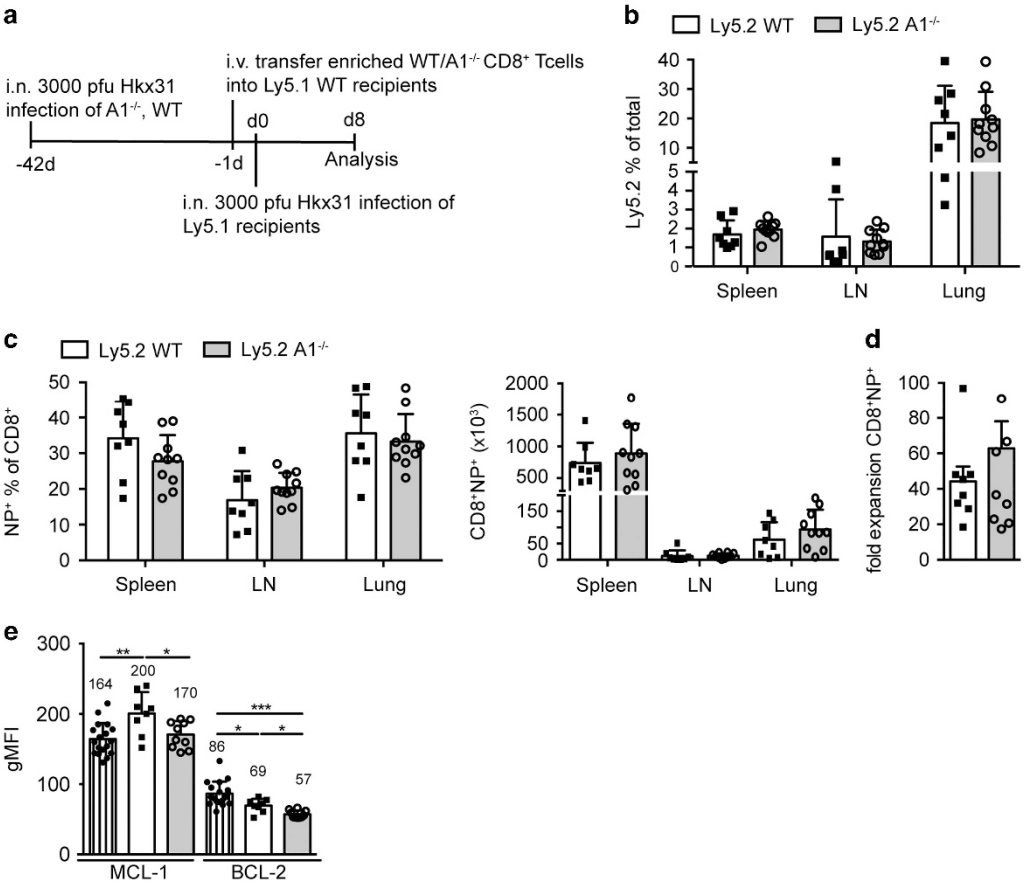

Figure 5 *A1*$^{-/-}$ T cells expand normally in an influenza rechallenging model. (**a**) Schematic overview of the influenza recall immune response workflow: wild-type and *A1*$^{-/-}$ mice were infected i.n. with 3000 pfu HKx31 influenza virus and after 41 days mice were killed and CD8$^+$ T cells were enriched by negative magnetic bead sorting. A total of 2×10^4 NP-specific CD8$^+$ T cells were transferred i.v. into naive C57BL/6-Ly5.1 wild-type recipient mice. One day later mice were infected i.n. with 3000 pfu HKx31 influenza and 8 days later lungs, mLN and spleens were isolated and analysed by flow cytometry. (**b**) The frequencies of Ly5.2$^+$ donor cells were analysed in the spleen, mLN and lung infiltrates. (**c**) The frequencies and total numbers of NP$^+$ antigen-specific Ly5.2$^+$CD8$^+$ T cells were analysed in the spleens, mLN, and lung infiltrates of infected mice. (**d**) The fold expansion of total Ly5.2$^+$CD8$^+$NP$^+$ T cells was calculated by comparing the numbers of injected Ly5.2$^+$CD8$^+$NP$^+$ T cells to the number of recovered Ly5.2$^+$CD8$^+$NP$^+$ T cells from spleen, mLN and lung. (**e**) Intracellular staining for MCL-1 and BCL-2 was performed on total spleen cells of infected mice and the geometric mean fluorescent intensity (gMFI) for MCL-1 and BCL-2 protein in Ly5.2$^+$CD8$^+$ donor T cells was compared with that from similarly stained Ly5.1$^+$CD8$^+$ host T cells. Bars represent means ± S.E.M. ($n = 8$–10). A Mann Whitney statistical test was performed, *$P < 0.05$, **$P < 0.01$, ***$P < 0.0001$

marrow, ELISpot assays were performed. No differences were observed in the production of low-affinity (NP16 binding) or high-affinity (NP2 binding) antibody secreting cells between the two genotypes (Figure 6e).

These results show that A1 on its own is not critical for the development of Tfh as well as GC B cells and PC during a T cell-dependent humoral immune response.

Discussion

We show that loss of A1 does not impair T cell immunity in a diverse set of experimental systems. We therefore conclude that A1 does not exert a unique role in T cells or B cells during immune responses. It remains possible that A1 has overlapping roles with other pro-survival BCL-2 family members controlling lymphocyte homoeostasis and activation.

The lack of an obvious phenotype was unexpected, as the levels of *A1* mRNA and protein were both rapidly increased in T cells on TCR/CD3 ligation or stimulation with mitogens[17,18,23] A1 induction has been defined as a central step in rewiring the cell survival machinery in T cells during the transition from a resting to an activated state. This is associated with a change from a cytokine receptor (mainly IL-7R) to a TCR-driven survival programme and includes the induction of BCL-XL and A1, accompanied by a down-regulation of BCL-2.[3] Therefore, it was surprising that *A1*$^{-/-}$ mice had no difficulties in clearance of an acute viral infection. Interestingly, T cell-specific loss of BCL-XL, which is also strongly induced on TCR/CD28 stimulation,[24] does not impair T cell responses to *Listeria monocytogenes* infection and humoral immune responses.[10] This may suggest functional redundancy between these two BCL-2-like proteins.

Besides exhaustion and subsequent inactivation of CTLs, BID- and BIM-dependent apoptosis occurs during persistent viral infection to regulate T cell shutdown.[25] Therefore, we examined whether A1 might be involved in the response to chronic LCMV infection. Surprisingly, we found neither a role for A1 in the overall immune response nor in the survival of

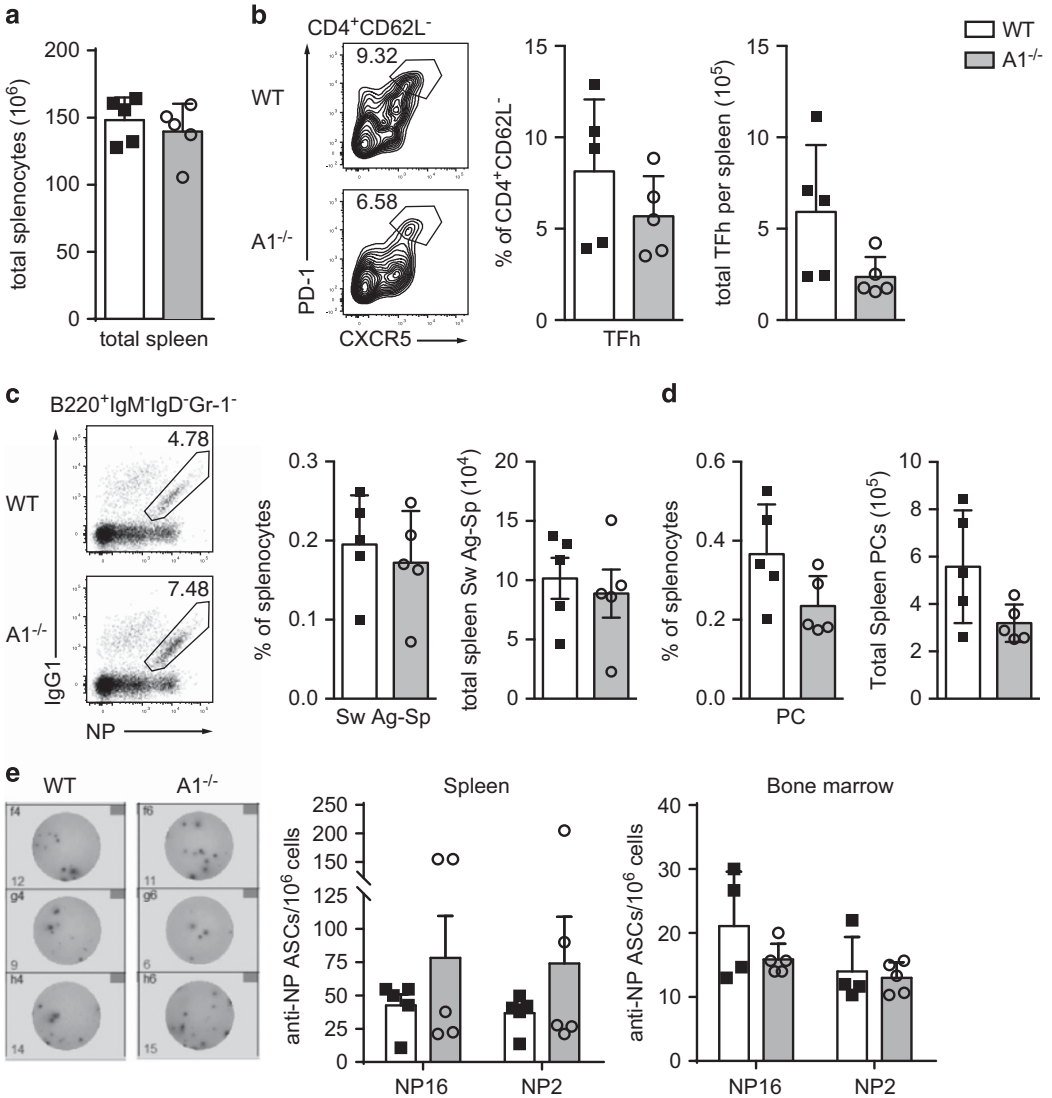

Figure 6 CD4 T-helper cell function is not impaired in $A1^{-/-}$ mice immunised with NP-KLH/Alum. (**a**) The numbers of total spleen cells of wild-type and $A1^{-/-}$ mice that had been immunised i.p. with 100 μg/20 g body weight NP-KLH/Alum 14 days earlier were determined. (**b**) The frequencies and total numbers of $CD4^+CXCR5^+PD\text{-}1^+$ Tfh cells in immunised wild-type and $A1^{-/-}$ mice were analysed by flow cytometry. (**c**) The numbers of $IgG1^+NP^+B220^+$ class-switched antigen-specific B cells and (**d**) $Syndecan1^+$ plasma cells in the spleen were determined by flow cytometry. (**e**) Overall, 1×10^6 spleen cells or bone-marrow cells were cultured overnight on NP16- or NP2-coated ELISA plates and ELISpot assays were performed. Antigen-specific plasma cells producing low (NP16) or high-affinity (NP2) antibodies against NP per 10^6 cells were quantified. Pictures show representative ELISpots from wild-type or $A1^{-/-}$ bone-marrow cells cultured overnight on NP2-coated ELISA plates. Bars represent means $\pm$ S.E.M. ($n = 5$)

high- as well as low-affinity T cell populations. These findings demonstrate that A1 is not essential for the development and survival of CTLs during persistent viral infection or for the preferential survival of high-affinity TCR bearing T cell clones. Our data further strengthen the notion that MCL-1 appears to be the only pro-survival BCL-2 family member that cannot be substituted by other BCL-2 pro-survival family members during T cell activation.[12]

A1 is readily detectable in memory T cells, and unchallenged $A1^{-/-}$ mice display a slight reduction in $CD4^+$ memory T cells.[17] These observations suggested a role for A1 as a survival factor for long-lived memory T cells that are still present after the termination of an anti-viral immune response. Although it has been shown that the BIM/BCL-2 axis is a main regulator of the formation and maintenance of memory T cells,[26,27] NOXA has also been proposed to have a role in regulating the size and clonal diversity of memory T cell populations.[5,28] This is of particular interest as NOXA, like A1, is induced transcriptionally after TCR ligation.[5] NOXA is believed to antagonise MCL-1 to set a threshold for the survival of those CTLs with high-affinity TCRs.[5] Accordingly, $Noxa^{-/-}$ mice have a higher number of antigen-specific CTLs and an increased memory compartment with higher clonal diversity on infection with influenza.[28] A1 is the closest pro-survival relative to MCL-1 and the only other described high-affinity binding partner of NOXA.[29] Although we could not observe any defects in the generation of antigen-specific memory T cells in response to influenza infection in $A1^{-/-}$

mice, we cannot exclude that the clonal repertoire of $A1^{-/-}$ T cells differs from that of wild-type T cells.

It will be interesting to test whether A1 loss can enhance the gene dosage-dependent phenotypes noted in mice lacking one allele of *Mcl-1*.[30,31] Along this line it is worth mentioning that such unilateral functional redundancy was also reported in mice that lack the BH3-only protein BMF on a BIM-deficient background. $Bmf^{-/-}$lymphocytes, such as pre-B cells, showed no or only minor resistance to apoptotic stimuli, but this resistance was massively increased on additional loss of even only one allele of *Bim,* exceeding resistance observed in $Bim^{-/-}$ cells.[32]

Given that Tregs require continuous TCR signalling for their maintenance and function,[33] it was surprising that we did not observe higher A1 protein levels in Tregs when compared with conventional T cells (Tcons). It has been reported that *A1* mRNA levels are high in splenic Tregs but even higher in thymic Tregs when compared with the expression observed in $CD4^+$ Tcons.[34] However, this was not demonstrated at the protein level in this study. Our results nonetheless support similar or even lower protein expression levels of A1 in Tregs compared with Tcons. Therefore, we can only speculate that tonic TCR signalling as received by Tregs leads to the posttranslational downregulation of A1, which is only visible at the protein level. Indeed, it has been shown before that A1 is tightly regulated by ubiquitin-dependent proteasomal degradation.[18,35] Future experiments of A1 protein stability in Tregs will show whether this hypothesis holds true. Interestingly, non-challenged $A1^{-/-}$ mice displayed a slight reduction in Tregs compared with wild-type mice.[17] However, this small difference was abolished on viral infection. This may imply a role for A1 in the survival of Tregs under homoeostatic conditions. Alternatively, after TCR/CD3 stimulation, Treg cell survival might depend exclusively on MCL-1.[36]

Using a conditional RNAi mouse model to knockdown A1 expression, Carrington *et al.*[37] showed that conventional DCs (cDCs), which are critical for certain immune responses, rely on A1 for their survival. Schenk *et al.*[17] also demonstrated that A1-deficient mice have reduced numbers of cDCs. However, the normal immune response of $A1^{-/-}$ mice to viral infections observed here leads us to the question whether A1 may only be an auxiliary to MCL-1 in cDC survival or whether there are A1-independent antigen-presenting cells that can take over the control of CTL-mediated immune responses in $A1^{-/-}$ mice. This question remains to be further investigated.

It is also noteworthy that the above mentioned and other RNAi-based A1-knockdown mouse models did not show any reductions in the numbers of mature, naive T cells or defects in T cell activation in culture. The lack of a T cell defect was originally ascribed to incomplete knockdown of A1 in activated T cells,[8,15] but our analysis here points towards functional redundancy between A1 and other pro-survival BCL-2 family members in the survival of quiescent as well as activated T cells.

In conclusion, we showed that A1 ablation is not sufficient to impair viral T cell immune responses in mice. It is, however, interesting that although A1 and BCL-XL are both highly induced in T cells in response to TCR and co-stimulatory signals that contribute to T cell survival,[38–40] the loss of neither impairs T cell function. This leaves the possibility that A1 and BCL-XL act in a redundant manner or are only of minor importance compared with the highly potent survival protein MCL-1. These questions can now be addressed by the generation of compound mutant mice lacking A1 and/or BCL-XL, BCL-2 and/or MCL-1 in mature T cells.

Materials and Methods

Mice. All experiments with mice were conducted according to the guidelines of The Walter and Eliza Hall Institute of Medical Research Animal Ethics Committee. $A1^{-/-}$ mice were generated on a C57BL/6 background.[17] Mice used for *in vivo* experiments were all 6–10 weeks of age. Bone-marrow (BM) chimaeras were generated by reconstitution of lethally irradiated recipient mice (two doses of 5.5 Gy, 3 h apart) with a mixture of $A1^{-/-}$ or wild-type bone marrow (Ly5.2) and isogenic wild-type bone marrow (Ly5.1). Mice were analysed 8-12 weeks post reconstitution. $Foxp3^{YFP\text{-}cre}$ mice[41] were used for sorting wild-type Treg cells based on YFP expression.

***In vitro* T cell activation.** $CD4^+$ and $CD8^+$ T cells were FACS-sorted from spleens of wild-type mice and cultured in RPMI1640 medium supplemented with 10% foetal calf serum (FCS, PAA, Pasching, Austria, FBS Gold #A15-151), 2 mM l-Glutamine, 1% Penicillin plus Streptomycin (10.000 U/ml Penicillin, 10 mg/ml Streptomycin in 0.9% NaCl) and 50 μg/ml Gentamicin. T cells were activated with 5 μg/ml plate-bound anti-CD3 (BioLegend, San Diego, CA, USA, clone 145-2C11) and 1 μg/mL anti-CD28 (BioLegend, clone 37.51) antibodies for the indicated time points.

LCMV infection. LCMV infections were performed by injection of 2×10^6 pfu LCMV docile into the tail vein of mice. The origin and biology of LCMV docile has been described.[21] This virus was propagated in L929 cells.

To analyse the cytokine production in response to restimulation of LCMV-specific cells, 1×10^6 total splenocytes were cultured overnight in the presence of 10-8 M LCMV GP33 (sequence KAVYNFATM), LCMV NP396 (sequence FQPQNGQFI), or non-stimulatory adenovirus (SGPSNTPPEI) in the presence of the protein transport inhibitor Monensin (BD Biosciences, Franklin Lakes, NJ, USA) and stained thereafter for cytokine production as described below.

Viral titres were analysed using the LCMV focus forming assay as described before.[42] In short, brain, liver, lung, spleen and kidney were collected in MEM 2% FCS and frozen at -80 °C before further analysed. Organs were homogenised and supernatant dilutions were used to infect monolayers of MC57 cells (8×10^5 per ml), Cells were overlayed with 2% methyl cellulose (Fluka #64620) in DME and plates were incubated at 37 °C, 5% CO_2 for 48 h. Viral plaque staining was performed after fixation of the cells with 4% Formalin-PBS and permeabilization with 0.1% Triton X (FLUKA #93418) with VL-4 rat anti-LCMV monoclonal antibody (WEHI Antibody Facility, Melbourne, VIC, Australia) followed by Peroxidase-conjugated AffiniPure goat anti-rat IgG (H+L) antibodies (Jackson ImmunoResearch Laboratories, West Grove, PA, USA #112-035-003). A colour-reaction of ortho-phenylendiamin (Sigma-Aldrich, Pty. Ltd. Sydney, Australia, #P3888) substrate was used for detection of focus forming units. The focus forming unit was used to calculate the viral titre in the original supernatant.

Influenza HKx31 Infection. Mice were lightly anaesthetised by inhalation of methoxyflurane, and infected i.n. with 3000 pfu of HKx31 (H3N2) influenza virus[43] in 25 μl PBS. Virus stocks were grown in the allantoic cavity of 10 day old embryonated chicken eggs, from which the viral titre was determined by plaque assay on monolayers of Madin Derby canine kidney (MDCK) cells.

Infiltrates from the lung were isolated as follows: lungs were mashed through 70 μm cell strainers (BD Biosciences, Cat# 352350) and washed with PBS. Pellets were resuspended in 5 ml PBS supplemented with 2% FCS and underlayed with 3 ml Histopaque 1083 (Sigma, Cat# 1083-1) followed by 30 min centrifugation at 400x*g* at room temperature with the brakes set off. Mononuclear cells were isolated from the opaque interface and washed extensively with PBS. Staining for cell surface and intracellular markers was performed as described below.

Enrichment of $CD8^+$ CTLs for influenza rechallenging model. For the enrichment of $CD8^+$ CTLs from spleens of infected mice, splenocytes were incubated with supernatants from hybridoma clones producing the following mABs (WEHI, Antibody Facility, Melbourne, VIC, Australia): rat anti-B220, rat anti-CD11b, rat anti-GR-1, rat anti-CD4, and rat anti-MHCII. Spleen cells expressing these

surface markers were depleted using goat anti-rat IgG antibody conjugated magnetic beads (NEB, Ipswich, MA, USA, Cat# S1433S). Enrichment efficiency was assessed by flow cytometry and 2×10^4 NP-specific CTLs were injected in 200 μl PBS i.v. into Ly5.1 wild-type recipient mice.

T lymphocyte-dependent B cell immune responses. Mice were immunised by i.p. injection of 100 μg/20 g body weight of 4-hydroxy-3-nitrophenylacetyl (NP) coupled to Keyhole Limpet Hemocyanin (KLH) at a ratio of 27 : 1 and precipitated onto alum.[44] Mice were sacrificed 14 days post immunisation and spleen and bone marrow were isolated for analysis.

Enzyme-linked immunospot assay. The frequency of ASC was determined as described.[44] Briefly, cells were incubated O/N at 37 °C on pre-coated 96-well MultiScreen-HA filter plates (Merck Millipore, Bayswater, VIC, Australia). Spots were visualised with goat anti-mouse IgG1 antibodies conjugated to horseradish peroxidase (Southern Biotechnology Associates, Birmingham, AL, USA), and staining was performed with 3-amino-9-ethyl carbazole (Sigma-Aldrich). Plates were washed extensively, and spots were counted using an AID ELIspot reader system (Autoimmun Diagnostika, Strassberg, Germany).

Western blot analysis. Cells were lysed in lysis buffer (50 mM Tris pH 8, 150 mM NaCl, 0.5% NP-40, 50 mM NaF, 1 mM Na_3VO_4, 1 mM PMSF, one tablet protease inhibitors (EDTA free, Roche Austria, Vienna, Austria) per 10 ml and 30 μg/ml DNaseI (Sigma-Aldrich, St. Louis, MO, USA) and protein was quantified with Bradford reagent (500-0006, Bio-Red, Munich, Germany). Overall, 30 μg total protein was loaded on 12% Bis-Tris acryl-amide gels and blotted on AmershamTM HybondTM-ECL nitrocellulose membranes (GE Healthcare, Little Chalfont, UK). The following antibodies were used for protein detection: rat anti-mouse A1 (6D6, 2 μg/ml),[18] rat anti-BIM (WEHI Antibody Facility, Melbourne, VIC, Australia, clone 3C5, 2.6 μg/ml), mouse anti-HSP90 (F8, Santa Cruz, Dallas, TX, USA, Cat# sc-13119, 0.2 μg/ml), rabbit anti-MCL-1 (polyclonal, Rockland, Limerick, PA, USA, Cat# 600-401-394, 2.2 μg/ml), rabbit anti-BCL-XL (54H6, Cell Signaling, Danvers, MA, USA, Cat# CS2764, 1:1000), rabbit anti-P38 MAPK (polyclonal, Cell Signaling Cat# 9212, 1:1000). All primary antibodies were diluted in 5% BSA in PBST and blots were incubated overnight at 4 °C.

mRNA purification and qRT-PCR analysis. RNA from approximately 1×10^5 cells was isolated, using the Quick-RNA MicroPrep (Zymo Research, Irvine, CA, USA, #R1051) and up to 200 ng RNA was used to generate cDNA using the iScript cDNA Synthesis Kit (Bio-Rad #170-8891).

qRT-PCR was performed using Platinum SYBR Green qPCR SuperMix-UDG reagent (Invitrogen, Waltham, MA, USA) and following primers: A1 fwd 5′ CCTGGCTGAGCACTACCTTC3′; A1 rev 5′TCCACGTGAAAGTCATCCAA3′; Mcl-1 fwd 5′TAACAAACTGGGGCAGGATT3′ Mcl-1 rev 5′GTCCCGTTTCGTCCTTACAA 3′; Bcl-xL fwd 5′TTCGGCATGGAGTAAACTGG3′ Bcl-xL rev 5′TGGATCCA AGGCTCTAGGTG3′; Bcl-2 fwd 5′CTGGCATCTTCTCCTTCCAG3′ Bcl-2 rev 5′ GACGGTAGCGACGAGAGAAG3′; and actin fwd 5′ACTGGGACGACATGGAGAAG 3′ actin rev 5′GGGGTGTTGAAGGTCTCAAA3′. PCR conditions: 7 min 95 °C; 40 cycles× (10 s 95 °C; 20 s 60 °C; 20 s 72 °C); 15 s on 95 °C; 15 s 60 °C; melting curve 20 min; 15 s 95 °C. Relative quantification was calculated using the $^{\Delta\Delta}$CT method.

Antibodies and flow cytometry. Fluorochrome-conjugated rat monoclonal antibodies directed against the following cell subset specific surface markers were used for flow cytometric analysis: CD4 (RM 4-5), CD62L (MEL-14), Ly5.2 (104), CD44 (IM7), Ly6C (AL-21), CD11b (M1/70), IgG1 (RMG1-1), GR1 (Ly6G/C), CD69 (H1.2F3), CD19 (1D3) from BD Pharmingen (Franklin Lakes, NJ, USA); CCR2 (#475301) from R&D (Minneapolis, MN, USA); ICOS (7E-17G9), PD-1 (J43), CD103 (2E7), KLRG1 (2F1), CD25 (PC61.5), Tigit (GIGD7), TCRβ (H57-597), CXCR3 (CXCR3-173), Ly5.1 (A20), ST2 (RMST2-2), Ly6C (HK1.4), GATA-3 (TWAJ), CD11c (N418), F4/80 (BM8), CD19 (MB19-1), CD127 (A7R34), CD8 (53-6.7) from eBioscience (San Diego, CA, USA); CXCR5 (L138D7), B220 (RA3-6B2), Syndecan (281-2) from BioLegend (San Diego, CA, USA); NP-PE from Biosearch Technologies (Steinach-Thur, Germany, #N-5070-1).

Intracellular staining of FoxP3 (eBioscience, clone FJK-16 s, 0.1 μg/ml) was performed using the eBioscience FOXP3 staining kit (Cat# 00-5523-00) according to the manufacturer's protocol. Intracellular staining for fluorochrome-conjugated IFN-γ (eBioscience, clone XMG1.2, 0.1 μg/ml), MCL-1 (clone 19C4-15, 0.5 μg/ml)[45] and BCL-2 (BD biosciences, clone 3F11, 1:200) was performed using the BD Cytofix/Cytoperm Fixation/Permeabilization kit (Cat# 554714) according to the manufacturer's protocol.

Influenza virus (HKx31)-specific responses were quantified by staining with phycoerythrin-labelled of major histocompatibility complex (MHC) class I tetrameric complexes specific for the H-2^b-restricted immunodominant epitope of influenza virus: NP366 (H-2D^b). LCMV-specific CD8$^+$ T cells were quantified with allophycocyanin-coupled tetramers MHC class I (H-2D^b) in complex with LCMV GP33 (sequence KAVYNFATM), or NP396 (sequence FQPQNGQFI) (Baylor College Medicine, Houston, TX, USA).

Antibody-stained cells were analysed in a BD Fortessa1 or BD Fortessa X20. Cell sorting was performed using a BD FacsAriaTMIII Cell sorter (all BD Biosciences).

Statistical analysis. If not indicated differently, statistical analyses were conducted using a two-tailed Student's *t* test with Prism v.5.03 software (GraphPad, La Jolla, CA, USA). Data are shown as mean $\pm$ S.E. with *P*-values of < 0.05 considered statistically significant.[46–50]

Conflict of Interest

The authors declare no conflict of interest.

Acknowledgements. We thank all members of the Herold laboratory for their support and advice. G Siciliano, H Johnsons and their team for animal husbandry; S Monard and his team for help with flow cytometry; and D Tischner for help with RNA analysis. This work was supported by a Leukemia Foundation National Research Program PhD Scholarship (to RS), National Health and Medical Research Council, Australia (programme grant 1016701 and fellowship 1020363, to AS), project grant APP1049720 (to MJH). This work was made possible through Victorian State Government Operational Infrastructure Support and Australian Government National Health and Medical Research Council Independent Research Institutes Infrastructure Support Scheme. This work was supported by grants from the Austrian Science Fund (FWF), Grant I1298 (FOR-2036), the MCBO Doctoral College 'Molecular Cell Biology and Oncology' (W1101) and the 'Österreichische Krebshilfe Tirol'. MDH and ST are supported by a DOC-fellowship from the Austrian Academy of Science (ÖAW).

Author contributions

ST performed experiments, analysed data, wrote paper and prepared figures; RS performed experiments, analysed data and prepared figures; AV, MDH, SP, and DZ performed experiments and analysed data; AV and AS planned study design and edited paper, MJH conceived and planned study, and wrote paper.

1. Tan JT, Dudl E, LeRoy E, Murray R, Sprent J, Weinberg KI *et al.* IL-7 is critical for homeostatic proliferation and survival of naive T cells. *Proc Natl Acad Sci USA* 2001; **98**: 8732–8737.
2. Opferman JT, Letai A, Beard C, Sorcinelli MD, Ong CC, Korsmeyer SJ. Development and maintenance of B and T lymphocytes requires antiapoptotic MCL-1. *Nature* 2003; **426**: 671–676.
3. Koenen P, Heinzel S, Carrington EM, Happo L, Alexander WS, Zhang JG *et al.* Mutually exclusive regulation of T cell survival by IL-7 R and antigen receptor-induced signals. *Nat Commun* 2013; **4**: 1735.
4. Sandalova E, Wei CH, Masucci MG, Levitsky V. Regulation of expression of Bcl-2 protein family member Bim by T cell receptor triggering. *Proc Natl Acad Sci USA* 2004; **101**: 3011–3016.
5. Wensveen FM, van Gisbergen KP, Derks IA, Gerlach C, Schumacher TN, van Lier RA *et al.* Apoptosis threshold set by Noxa and Mcl-1 after T cell activation regulates competitive selection of high-affinity clones. *Immunity* 2010; **32**: 754–765.
6. Hildeman DA, Zhu Y, Mitchell TC, Bouillet P, Strasser A, Kappler J *et al.* Activated T cell death *in vivo* mediated by proapoptotic bcl-2 family member bim. *Immunity* 2002; **16**: 759–767.
7. Best JA, Blair DA, Knell J, Yang E, Mayya V, Doedens A *et al.* Transcriptional insights into the CD8(+) T cell response to infection and memory T cell formation. *Nat Immunol* 2013; **14**: 404–412.
8. Sochalska M, Ottina E, Tuzlak S, Herzog S, Herold M, Villunger A. Conditional knockdown of BCL2A1 reveals rate-limiting roles in BCR-dependent B cell survival. *Cell Death Differ* 2016; **23**: 628–639.
9. Nakayama K, Nakayama K, Negishi I, Kuida K, Shinkai Y, Louie MC *et al.* Disappearance of the lymphoid system in Bcl-2 homozygous mutant chimeric mice. *Science* 1993; **261**: 1584–1588.
10. Zhang N, He YW. The antiapoptotic protein Bcl-xL is dispensable for the development of effector and memory T lymphocytes. *J Immunol* 2005; **174**: 6967–6973.

11. Dzhagalov I, Dunkle A, He YW. The anti-apoptotic Bcl-2 family member Mcl-1 promotes T lymphocyte survival at multiple stages. *J Immunol* 2008; **181**: 521–528.
12. Tripathi P, Koss B, Opferman JT, Hildeman DA. Mcl-1 antagonizes Bax/Bak to promote effector CD4(+) and CD8(+) T cell responses. *Cell Death Differ* 2013; **20**: 998–1007.
13. Verschelde C, Walzer T, Galia P, Biemont MC, Quemeneur L, Revillard JP *et al.* A1/Bfl-1 expression is restricted to TCR engagement in T lymphocytes. *Cell Death Differ* 2003; **10**: 1059–1067.
14. Hatakeyama S, Hamasaki A, Negishi I, Loh DY, Sendo F, Nakayama K *et al.* Multiple gene duplication and expression of mouse bcl-2-related genes, A1. *Int Immunol* 1998; **10**: 631–637.
15. Ottina E, Lyberg K, Sochalska M, Villunger A, Nilsson GP. Knockdown of the antiapoptotic Bcl-2 family member A1/Bfl-1 protects mice from anaphylaxis. *J Immunol* 2015; **194**: 1316–1322.
16. Ottina E, Grespi F, Tischner D, Soratroi C, Geley S, Ploner A *et al.* Targeting antiapoptotic A1/Bfl-1 by *in vivo* RNAi reveals multiple roles in leukocyte development in mice. *Blood* 2012; **119**: 6032–6042.
17. Schenk RL, Tuzlak S, Carrington EM, Zhan Y, Heinzel S, Teh CE *et al.* Characterisation of mice lacking all functional isoforms of the pro-survival BCL-2 family member A1 reveals minor defects in the haematopoietic compartment. *Cell Death Differ* 2016 (in press; doi:10.1038/cdd.2016.156).
18. Lang MJ, Brennan MS, O'Reilly LA, Ottina E, Czabotar PE, Whitlock E *et al.* Characterisation of a novel A1-specific monoclonal antibody. *Cell Death Dis* 2014; **5**: e1553.
19. Mandal M, Borowski C, Palomero T, Ferrando AA, Oberdoerffer P, Meng F *et al.* The BCL2A1 gene as a pre-T cell receptor-induced regulator of thymocyte survival. *J Exp Med* 2005; **201**: 603–614.
20. Tomayko MM, Punt JA, Bolcavage JM, Levy SL, Allman DM, Cancro MP. Expression of the Bcl-2 family member A1 is developmentally regulated in T cells. *Int Immunol* 1999; **11**: 1753–1761.
21. Moskophidis D, Lechner F, Pircher H, Zinkernagel RM. Virus persistence in acutely infected immunocompetent mice by exhaustion of antiviral cytotoxic effector T cells. *Nature* 1993; **362**: 758–761.
22. Swain SL, McKinstry KK, Strutt TM. Expanding roles for CD4+ T cells in immunity to viruses. *Nat Rev Immunol* 2012; **12**: 136–148.
23. Grumont RJ, Rourke IJ, Gerondakis S. Rel-dependent induction of A1 transcription is required to protect B cells from antigen receptor ligation-induced apoptosis. *Genes Dev* 1999; **13**: 400–411.
24. Groux H, Monte D, Plouvier B, Capron A, Ameisen JC. CD3-mediated apoptosis of human medullary thymocytes and activated peripheral T cells: respective roles of interleukin-1, interleukin-2, interferon-gamma and accessory cells. *Eur J Immunol* 1993; **23**: 1623–1629.
25. Masson F, Kupresanin F, Mount A, Strasser A, Belz GT. Bid and Bim collaborate during induction of T cell death in persistent infection. *J Immunol* 2011; **186**: 4059–4066.
26. Wojciechowski S, Tripathi P, Bourdeau T, Acero L, Grimes HL, Katz JD *et al.* Bim/Bcl-2 balance is critical for maintaining naive and memory T cell homeostasis. *J Exp Med* 2007; **204**: 1665–1675.
27. Kurtulus S, Tripathi P, Moreno-Fernandez ME, Sholl A, Katz JD, Grimes HL *et al.* Bcl-2 allows effector and memory CD8+ T cells to tolerate higher expression of Bim. *J Immunol* 2011; **186**: 5729–5737.
28. Wensveen FM, Klarenbeek PL, van Gisbergen KP, Pascutti MF, Derks IA, van Schaik BD *et al.* Pro-apoptotic protein Noxa regulates memory T cell population size and protects against lethal immunopathology. *J Immunol* 2013; **190**: 1180–1191.
29. Chen L, Willis SN, Wei A, Smith BJ, Fletcher JI, Hinds MG *et al.* Differential targeting of prosurvival Bcl-2 proteins by their BH3-only ligands allows complementary apoptotic function. *Mol Cell* 2005; **17**: 393–403.
30. Delbridge AR, Opferman JT, Grabow S, Strasser A. Antagonism between MCL-1 and PUMA governs stem/progenitor cell survival during hematopoietic recovery from stress. *Blood* 2015; **125**: 3273–3280.
31. Grabow S, Delbridge AR, Valente LJ, Strasser A. MCL-1 but not BCL-XL is critical for the development and sustained expansion of thymic lymphoma in p53-deficient mice. *Blood* 2014; **124**: 3939–3946.
32. Labi V, Woess C, Tuzlak S, Erlacher M, Bouillet P, Strasser A *et al.* Deregulated cell death and lymphocyte homeostasis cause premature lethality in mice lacking the BH3-only proteins Bim and Bmf. *Blood* 2014; **123**: 2652–2662.
33. Vahl JC, Drees C, Heger K, Heink S, Fischer Julius C, Nedjic J *et al.* Continuous T cell receptor signals maintain a functional regulatory T cell pool. *Immunity* 2014; **41**: 722–736.
34. Tischner D, Gaggl I, Peschel I, Kaufmann M, Tuzlak S, Drach M *et al.* Defective cell death signalling along the Bcl-2 regulated apoptosis pathway compromises Treg cell development and limits their functionality in mice. *J Autoimmun* 2012; **38**: 59–69.
35. Herold MJ, Zeitz J, Pelzer C, Kraus C, Peters A, Wohlleben G *et al.* The stability and anti-apoptotic function of A1 are controlled by its C terminus. *J Biol Chem* 2006; **281**: 13663–13671.
36. Pierson W, Cauwe B, Policheni A, Schlenner SM, Franckaert D, Berges J *et al.* Antiapoptotic Mcl-1 is critical for the survival and niche-filling capacity of Foxp3(+) regulatory T cells. *Nat Immunol* 2013; **14**: 959–965.
37. Carrington EM, Zhang JG, Sutherland RM, Vikstrom IB, Brady JL, Soo P *et al.* Prosurvival Bcl-2 family members reveal a distinct apoptotic identity between conventional and plasmacytoid dendritic cells. *Proc Natl Acad Sci USA* 2015; **112**: 4044–4049.
38. Rogers PR, Song J, Gramaglia I, Killeen N, Croft M. OX40 promotes Bcl-xL and Bcl-2 expression and is essential for long-term survival of CD4 T cells. *Immunity* 2001; **15**: 445–455.
39. Song J, Salek-Ardakani S, Rogers PR, Cheng M, Van Parijs L, Croft M. The costimulation-regulated duration of PKB activation controls T cell longevity. *Nat Immunol* 2004; **5**: 150–158.
40. Lei F, Song J, Haque R, Haque M, Xiong X, Fang D *et al.* Regulation of A1 by OX40 contributes to CD8(+) T cell survival and anti-tumor activity. *PLoS ONE* 2013; **8**: e70635.
41. Rubtsov YP, Rasmussen JP, Chi EY, Fontenot J, Castelli L, Ye X *et al.* Regulatory T cell-derived interleukin-10 limits inflammation at environmental interfaces. *Immunity* 2008; **28**: 546–558.
42. Wang C, McPherson AJ, Jones RB, Kawamura KS, Lin GH, Lang PA *et al.* Loss of the signaling adaptor TRAF1 causes CD8+ T cell dysregulation during human and murine chronic infection. *J Exp Med* 2012; **209**: 77–91.
43. Flynn KJ, Belz GT, Altman JD, Ahmed R, Woodland DL, Doherty PC. Virus-specific CD8+ T cells in primary and secondary influenza pneumonia. *Immunity* 1998; **8**: 683–691.
44. Smith KG, Light A, Nossal GJ, Tarlinton DM. The extent of affinity maturation differs between the memory and antibody-forming cell compartments in the primary immune response. *EMBO J* 1997; **16**: 2996–3006.
45. Campbell KJ, Bath ML, Turner ML, Vandenberg CJ, Bouillet P, Metcalf D *et al.* Elevated Mcl-1 perturbs lymphopoiesis, promotes transformation of hematopoietic stem/progenitor cells, and enhances drug resistance. *Blood* 2010; **116**: 3197–3207.
46. Czabotar PE, Lessene G, Strasser A, Adams JM. Control of apoptosis by the BCL-2 protein family: implications for physiology and therapy. *Nat Rev Mol Cell Biol* 2014; **15**: 49–63.
47. Llambi F, Wang YM, Victor B, Yang M, Schneider DM, Gingras S *et al.* BOK Is a non-canonical BCL-2 family effector of apoptosis regulated by ER-associated degradation. *Cell* 2016; **165**: 421–433.
48. Ke F, Voss A, Kerr JB, O'Reilly LA, Tai L, Echeverry N *et al.* BCL-2 family member BOK is widely expressed but its loss has only minimal impact in mice. *Cell Death Differ* 2012; **19**: 915–925.
49. Chipuk JE, Green DR. How do BCL-2 proteins induce mitochondrial outer membrane permeabilization? *Trends Cell Biol* 2008; **18**: 157–164.
50. Thomas LW, Lam C, Edwards SW. Mcl-1; the molecular regulation of protein function. *FEBS Lett* 2010; **584**: 2981–2989.

Supplementary Information accompanies this paper on *Cell Death and Differentiation* website (http://www.nature.com/cdd).